Piezoresistive cantilevers utilized for scanning tunneling and scanning force microscope in ultrahigh vacuum

F. J. Giessibl and B. M. Trafas

Piezoresistive cantilevers utilized for scanning tunneling and scanning force microscope in ultrahigh vacuum

F. J. Giessibl and B. M. Trafas
Park Scientific Instruments, 1171 Borregas Avenue, Sunnyvale, California 94089

Piezoresistive cantilevers have been utilized in a novel ultrahigh vacuum scanning probe microscope which allows *in situ* scanning tunneling microscopy (STM), contact atomic force microscopy (AFM), and noncontact atomic force microscopy. The instrument uses interchangeable tungsten tips (for STM imaging) and piezoresistive cantilevers (for AFM or STM imaging) and is capable of atomic resolution in both STM and AFM modes of operation. *In situ* tip exchange under vacuum conditions is performed quickly and reliably using a high precision rotary/linear feedthrough and a tip/cantilever storage system. Piezoresistive force-sensing cantilevers provide a new detection scheme for AFM, using an all-electronic detector that requires no alignment or optical detection system. The microscope features a high-resolution, dual-axis, inertial-drive translation stage with an open access sample mount designed to optimize vibration isolation.

I. INTRODUCTION

In the development of scanning tunneling microscopy (STM) for ultrahigh vacuum (UHV), atomic scale imaging of the Si (111) 7×7 reconstruction was an important milestone.[1] Since then, many commercial and homebuilt instruments have demonstrated this capability. Further development of UHV STM instruments has focussed on improving the ease of use, decreasing the noise level, increasing flexibility in terms of sample holder sizes and weights, developing low and high temperature modes, and providing means for *in situ* tip preparation.

In recent years, interest in atomic force microscopy (AFM) in UHV has been increasing due to the ability of AFM in UHV to image nonconducting samples prepared in a controlled environment. The main obstacles preventing large scale AFM studies in UHV were the experimental difficulties involved in operating an AFM in vacuum. Until now, UHV atomic force microscopes have used vacuum tunneling,[2,3] capacitance sensor,[4] optical interferometry,[5] and optical lever detection[6–8] to detect changes in force between the sample and the cantilever tip. These methods all require a sensing element that is external to the cantilever. Due to the small size of the cantilever, transfer of a cantilever, and alignment of a laser beam or tunneling tip in vacuum is difficult. Other problems concern the requirement for bake-out and UHV compatibility of the light source in an optical beam deflection system, as well as tip stability and avoidance of contamination in tunneling detection schemes. All factors considered, it is difficult to design and operate an AFM in vacuum.

The recent development of the piezoresistive cantilever[9] provides an alternative detection scheme in which the detector is integrated in the cantilever. Integral force sensing has made it much easier to perform AFM in adverse environments such as UHV.

We have developed a UHV instrument which is capable of STM, contact AFM, and noncontact AFM. The instrument allows quick and easy interchange of the scanning probe, which is attached to the end of a piezoelectric tube scanner, and eliminates the need for precision alignment required for optical detection systems. The probe is either a tunneling tip (such as tungsten or platinum) or a piezoresistive cantilever mounted on a magnetic holder.

II. INSTRUMENT DESIGN

A schematic top down view of the instrument is shown in Fig. 1. The microscope is constructed on a standard 8 in. vacuum flange and includes a built-in vibration isolation stage consisting of a double spring suspension with eddy current damping.[10] The vibration isolation stage can be locked during tip and sample transfer. The instrument wiring is routed through two UHV 10-pin feedthroughs in order to separate the tunneling current and the force signal from the high-voltage control signals for the piezoelectric tube scanner and the translation stage. The wiring is carefully routed and attached to the outer stage of the vibration isolation stage to minimize the transmission of vibrations. The preamplifier for the tunneling current and the force signal is mounted directly outside the vacuum flange. The electrical connections to the tip, cantilever, and sample are therefore all directly accessible from outside vacuum. Removal of the preamplifier outside vacuum allows for *in situ* tip preparation methods like field emission without preamplifier damage.

The sample stage is a high-resolution, dual-axis, inertial-drive translation stage.[11] An open access sample mount can accommodate various sample holders up to a maximum weight of 150 g. The range of motion of the sample stage is 20 mm in the z direction and 7 mm in the x direction. The step size ranges between 50 and 250 nm and can be adjusted by changing the amplitude of the driving signal. The stage consists of a bottom, middle, and top level. The middle level contains three sapphire balls mounted on each side and has a magnet at its center. The top and bottom levels each contain one V-shaped and one flat groove. On each side of the middle level two of the sapphire balls travel in the V groove, and one travels over the flat groove, thereby forming a rigid cinematic mount. The grooves are furnished with alumina strips in order to establish a smooth surface and a constant
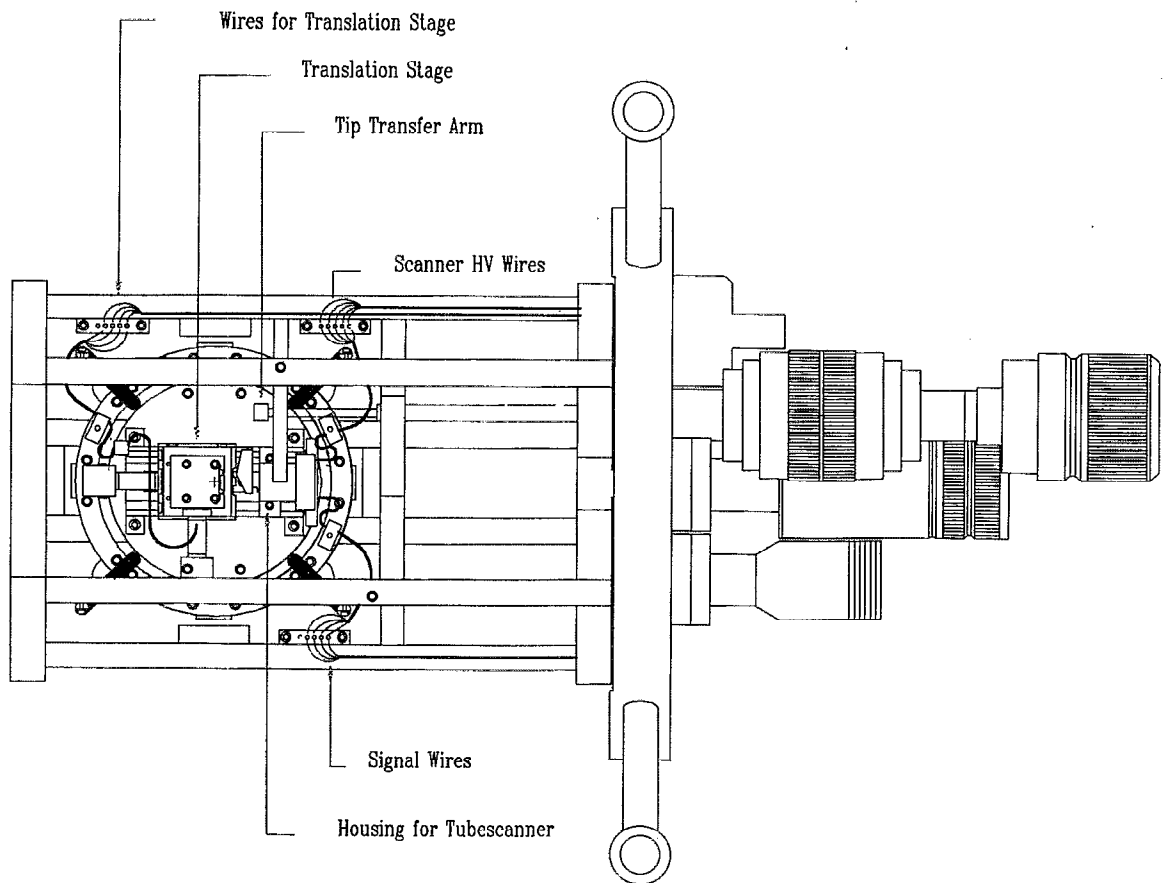
FIG. 1. Schematic showing a top down view of the instrument.

coefficient of friction. Both the top and bottom levels contain a central mounted μ-metal strip to couple to the magnet mounted in the middle level. This magnet is strong enough to hold the stage assembly together even when the stage is upside down. Metal clamps between the individual stage levels are provided to limit the travel length.

The scanner is of the piezoelectric tube type[12] and has a scanning range of 10 μm in the $x-y$ directions and 2.5 μm in the z direction. The free end of the scanner tube holds a magnetic coupling device that is used for probe exchange. The device includes three isolated electrical contacts. One of the contacts is used for the tunneling current, the other two are needed by the piezoresistive cantilever. A high-precision rotary/linear feedthrough with an attached fork and spring is used to facilitate transfer of a tip holder (or cantilever holder) from a probe storage carousel. The storage carousel holds up to six probes (both AFM cantilevers and STM tips). Switching between STM and AFM *in situ* takes less than 2 min including locking and unlocking the vibration isolation stage.

The software includes both data acquisition and image processing capabilities and uses a 66 MHz, 486 computer workstation running under the Windows 3.1 and MS-DOS 5 operating systems. The control electronics are DSP-based with six 18-bit DACs, four 18-bit ADCs, and a total of 24 multiplexed channels.

III. RESULTS AND DISCUSSION

Great emphasis has been placed in the development of this instrument on achieving mechanical stability, high ambient noise rejection, and low thermal drift rates. The rigidity of the instrument, together with the double-stage spring suspension system, enables us to obtain atomically resolved images even when mechanical/turbo pumps are running and vibrations of the vacuum chamber can be sensed by touching.

Figure 2 shows unprocessed data from a 195×195 Å^2 STM image of the Si(111)−7×7 surface taken with a tungsten tip. The sample was prepared by annealing to ~1200 °C. The image was taken at −1.96 V bias, tunneling from the tip to unoccupied sample states with a tunneling current of 0.4 nA. The acquisition rate in constant current mode at atomic resolution is approximately 2000 Å/s with either 256×256 or 512×512 data points per image. The significance of the STM image of Si(111) 7×7 presented here is to demonstrate the vertical and horizontal resolution, low thermal drift rates, and low noise and vibration levels. The acquisition software also includes $I-V$ spectroscopy for gathering detailed information about the electronic states on a surface.

The piezoresistive cantilever consists of a single crystal silicon structure with a diffused conductive channel and an
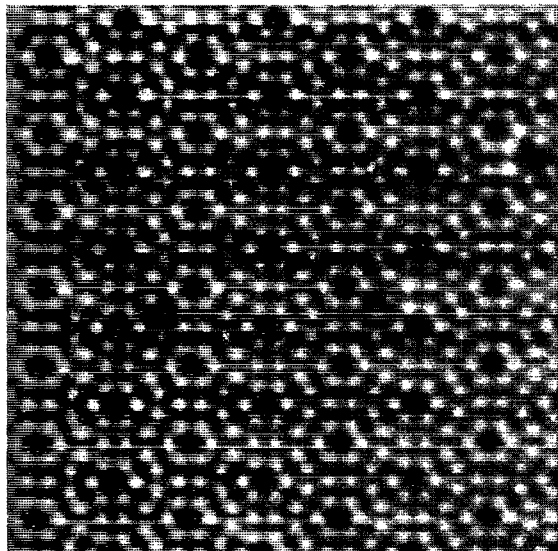
FIG. 2. Unfiltered STM image of Si(111) 7×7 for an area of 195×195 Å². The image was taken in constant current (topographic) mode at a sample bias of +1.96 V and a tunneling current 0.4 nA.

integrated ultrasharp asymptotic silicon tip (see SEM micrographs in Figs. 3(a) and 3(b)]. Deflection of the cantilever alters the resistance of the conductive channel (the piezoresistive effect). Figure 3(c) shows a schematic diagram of the piezoresistive detection scheme for AFM.[13] In our implementation, two electrical contacts on the piezoresistive cantilever connect it to an external dc-biased Wheatstone bridge which directly measures the deflection by measuring the change in the cantilever resistance. The conductive channel and the metal film resistors in the Wheatstone bridge have a resistance of 2 kΩ. The sensitivity S (relative change of resistance $\Delta R/R$ per Å of deflection) of the cantilevers is $0.3(\pm0.1)\times10^{-6}$ Å^{-1} at dc.[14] The output of the bridge is amplified by an AD 624 Instrumentation Amplifier[15] which is wired for a gain of $G=100$. The signal-to-noise ratio (SNR) of this detection scheme is high enough to measure the amplitude of the thermally excited eigenmode of the piezolevers at room temperature. The output voltage U_{out} of the bridge at deflection ζ is given by

$$U_{\text{out}}=0.25GU_0S\zeta. \qquad (1)$$

Figure 3(d) shows the spectrum of the detector output for a piezolever with a force constant of 2.5 N/m. Thermal excitation at room temperature should result in an amplitude of $\zeta_{\text{rms}}=0.4$ Å (calculated by applying the equipartition theorem: $\frac{1}{2}k_BT=\frac{1}{2}k\langle\zeta^2\rangle$). The total gain was $G=1000$, the full voltage across the bridge $U_0=10.0$ V. The rms amplitude of the output at the resonance frequency of the piezolever should be 300 μV. The integrated rms amplitude between the dotted lines in Fig. 3(d) is 264 μV, i.e., the sensitivity S [$0.3(\pm0.1)\times10^{-6}$ Å^{-1}] of the piezolevers is within the specified range not only at dc, but also at the eigenfrequency. The Q factor of the levers in vacuum is 28000, as determined by the full width at $1/\sqrt{2}$ maximal amplitude [i.e., full-width at half-maximum (FWHM) of the power spectrum, $Q=$eigenfrequency/FWHM]. Smith has done extensive measure-

ments on the piezolevers in UHV and at low temperatures and found that the SNR is even better at low temperatures.[16] We were operating the Wheatstone bridge at $U_0=2.5$ V and $U_0=10.0$ V. The heat dissipation $P_{\text{el}}=U_0^2/4R$ due to the electrical current in the piezolever should rise its temperature. We did not measure the temperature change directly, but we did record the eigenfrequency of the lever at the two different bridge voltages. The eigenfrequency ν_0 of the lever changed from 56 867.5 to 56 793.5 Hz, a relative change of −0.13% when the heat dissipation was increased from 0.78 to 12.5 mW. The frequency change of the optical phonons in silicon at room temperature is approx. -4.2×10^{-5} K^{-1}.[17]
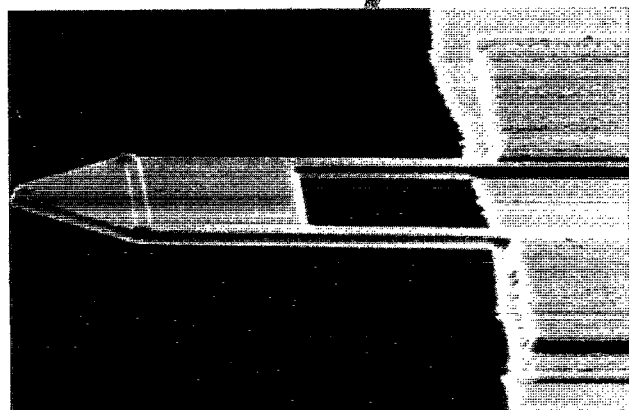
(a)
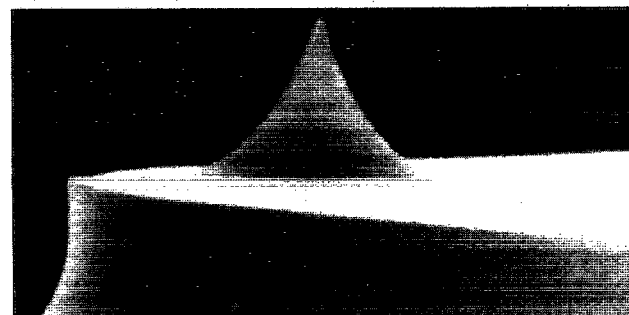
(b)
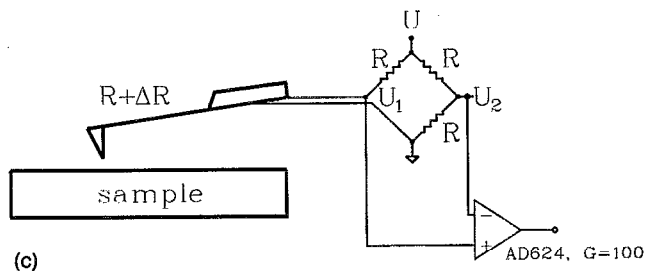
(c)

FIG. 3. (a) SEM micrograph of a piezoresistance cantilever. The protrusion at the end of the lever on the left side of the image is the integrated tip. The upper part of two legs of the piezolever is doped and changes its resistance when the lever is bent. The two squares in the right part of the image are electrical contacts that connect to metal traces. (b) Close-up view of the integrated silicon tip. The tip radius is approximately 4 nm. The integrated silicon tip can be used for STM as well if the native oxide is removed by field emission. (c) Schematic diagram of the piezolever detection scheme for AFM. The piezolever is part of a Wheatstone bridge, one of the legs is connected to ground, the other one to a metal film resistor with the same value (2 kΩ) and the input of an AD 624 instrumentation amplifier. The bridge voltage U_0 is either 2.50 or 10.0 V in our setup.

A: MAG

300
uVrms

30
uVrms
/DIV

0
Vrms

CENTER: 56 793.5 Hz   BW: 954.85 mHz   SPAN: 100 Hz
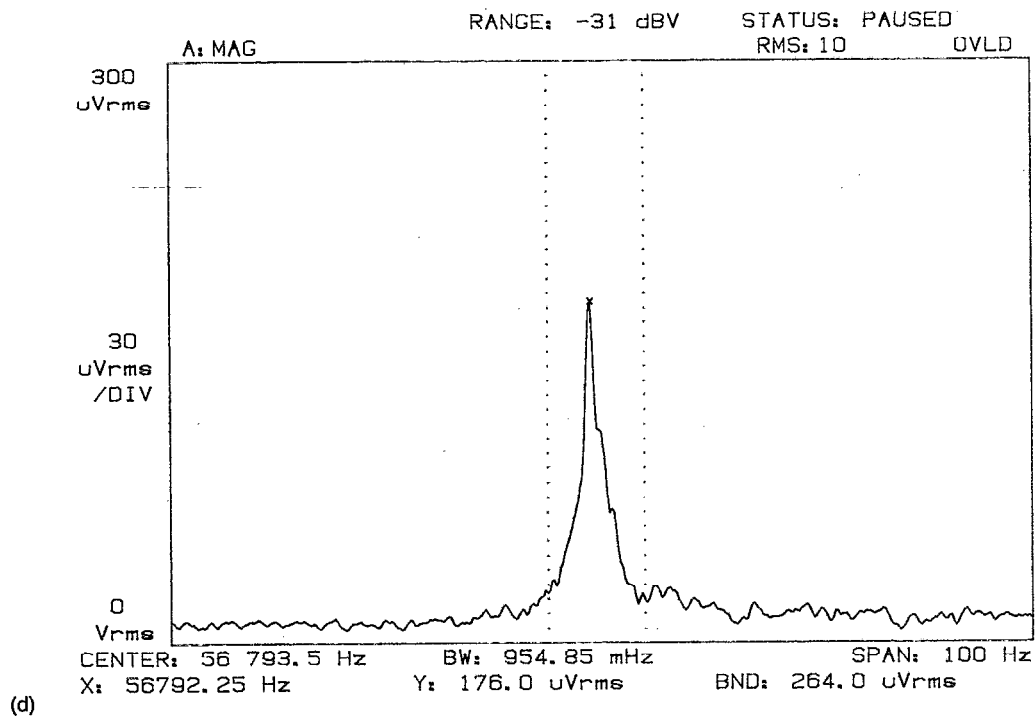X: 56792.25 Hz   Y: 176.0 uVrms   BND: 264.0 uVrms

(d)

FIG. 3. (d) Output of the bridge amplifier, amplified by a second amplifier to yield a total gain of 1000 when the piezolever was in UHV at room temperature. The peak corresponds to the thermally excited vibration of the piezolever at its lowest eigenmode. The bridge voltage U_0 is 10.0 V, the Q value as determined by dividing the eigenfrequency by the full-width at half-maximum of the power spectrum is 28 000.

Assuming, that the same elastic constants which determine the frequency of the optical phonons are responsible for the stiffness of the lever, the temperature increase is calculated to be 31 K. Assuming further, that the temperature rise is proportional to the power dissipation, the temperature increase for working at a bridge voltage $U_0 = 2.5$ V is only 2 K. The sample was far away from the piezolever and the piezolever was in UHV when the change in eigenfrequency was measured, i.e., the heat must have been transmitted to the substrate of the lever. The thermal coupling of the conductive channel to the substrate of the cantilever is obviously very good, as expected from the fact that the cantilever is made out of a single silicon crystal. The temperature rise is negligible for room temperature, and the heat which is dissipated by detecting the piezolever deflection is comparable or even less than in the case of optical detection, thus making piezolevers applicable at low temperatures.

The dc output of the Wheatstone bridge is used to drive the AFM feedback loop for contact mode. Figure 4 shows a 42×42 Å^2 contact AFM image of MoS$_2$ taken in ultrahigh vacuum. The topographic data are obtained at constant normal force. The image was collected using a piezoresistive cantilever with a calculated spring constant of 106 N/m and a minimum detectable deflection of 0.1 Å in the bandwidth from 10 Hz to 1 kHz. The nearest neighbor distance between features in the image is determined to be 3.0 Å, in agreement with expected values for MoS$_2$(0001). The significance of the atomic corrugations presented here is to demonstrate the sensitivity of the piezoresistive cantilever. In addition to these results, Tortonese et al. have shown atomic resolution imaging of graphite, boron nitride, molybdenum disulfide,

and tantalum disulfide using piezoresistive cantilevers in ambient conditions.[18]

We find that the resolution of the piezoresistive detection scheme is comparable to conventional optical lever AFM detection schemes and is more attractive due to its simplicity and reliability. The absence of external deflection sensing elements simplifies the design, and the low voltage dc response allows simple circuitry.
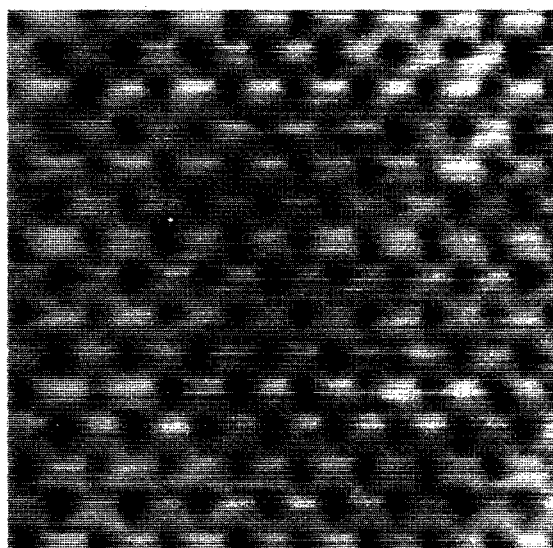
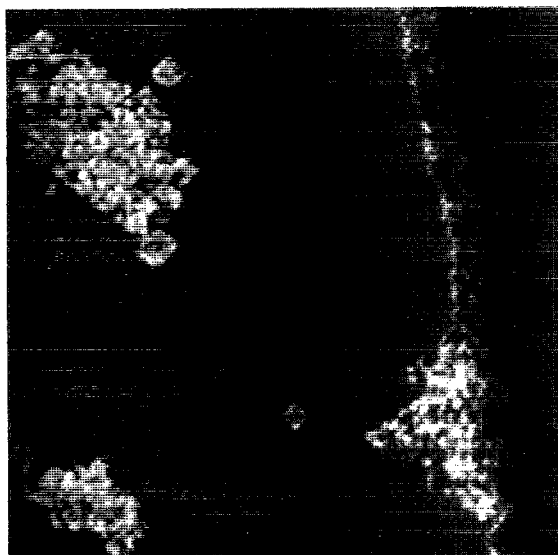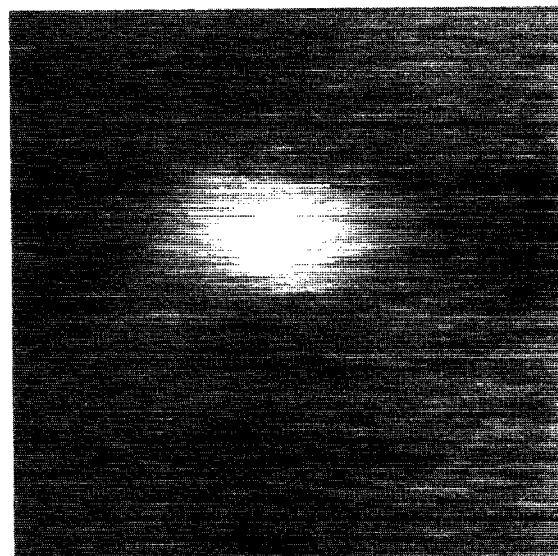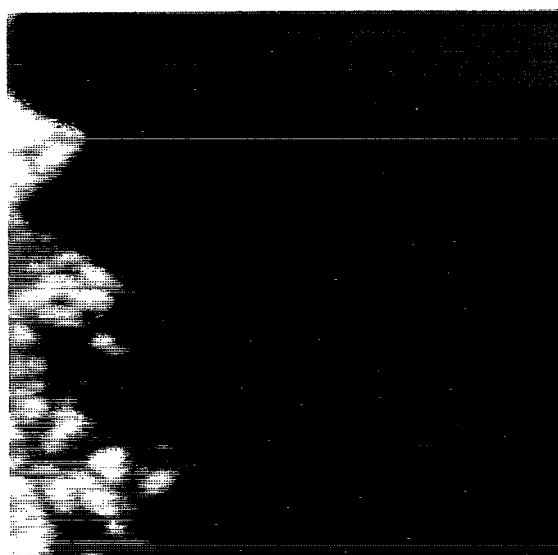We have also developed noncontact AFM using piezore-

FIG. 4. Contact mode AFM image of MoS$_2$ for an area of 42×42 Å^2 (nearest neighbor distance of 3 Å).

(a)

(b)

(c)

FIG. 5. (a) Noncontact AFM image of a cleavage face of KCl covering an area of 5000×5000 $Å^2$. (b) High resolution noncontact AFM image of the step structure of Fig. 5(a). The step heights are determined to be 3.1 and 6.2 Å in height. (c) Noncontact AFM image of a typical defect structure on the terraces of KCl. The circular structure is 30 Å in diameter and 1.5 Å in height.

sistive cantilevers, using FM detection that was pioneered by Albrecht et al.[19] In FM detection, the cantilever is driven at a fixed amplitude of vibration, and changes in its vibration frequency are detected. The FM detector measures much weaker force gradients than can be sensed using conventional AM detectors over a given bandwidth.[20]

Figure 5(a) shows a 5000×5000 $Å^2$ noncontact AFM image of KCl(001) taken in ultra high vacuum. The sample was cleaved in air and then transferred to vacuum. The image shows a [100] step structure running from the bottom to the top of the image. What makes this step structure of particular interest is that the step edges fluctuate around a mean position with kinks made up of steps in the ⟨110⟩ directions. The upper terrace region shows recrystallized islands bounded by these steps.

Figure 5(b) shows a second image of the step edge with a narrower scanwidth (1200×1200 $Å^2$). The majority of the steps are determined to be either 3.1 or 6.2 Å in height. The smallest measured step height corresponds to half a unit cell of KCl ($a_0/2$) and thus represents a monatomic step.

Examination of the terrace regions to the right and left of the step structure show several small defect features, which are typically 20–100 Å in diameter. Figure 5(c) shows a high resolution 100×100 $Å^2$ image of one of these defects. The defect is 30 Å in diameter and 1.5 Å in height. The defect structure represents a localized change in the attractive force between the cantilever tip and sample. We speculate that the change in attractive force is a localized electrostatic effect due to a charged defect in the KCl lattice structure.

To our knowledge, these images present some of the highest resolution images collected with a noncontact AFM system. Cross-sectional line measurements taken on the KCl step edges and measurements of the defect structures shown in Figs. 5(a) through 5(c) demonstrate that piezoresistive cantilevers operating in noncontact AFM are capable of resolving 1-atom high step edges with lateral resolution of ~30 Å.

In addition to these contact AFM and noncontact AFM results using piezoresistive cantilevers, we have recently demonstrated that piezoresistive cantilevers can be used to perform STM measurements. The piezoresistive cantilever is doped on one side and contains an integrated conducting tip.
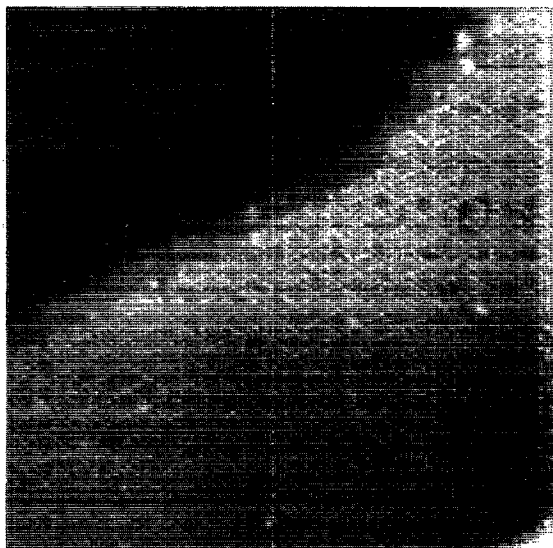
FIG. 6. Step on Si(111) 7×7 collected with a piezoresistive cantilever in STM mode. The image was acquired with a sample bias of −1.96 V and a tunneling current of 0.32 nA. The area imaged is 700×700 Å².

The cantilever may therefore be used to detect a tunneling current by biasing it and using the sharpened AFM tip as the tunneling probe. In this configuration, one electrical contact of the piezoresistance cantilever is grounded and the other electrical connection is connected to the bias voltage.

Figure 6 shows a 700×700 Å² constant current STM image of Si(111) 7×7 taken using a piezoresistive cantilever. The cantilever tip potential was −1.96 V and the tunneling current 0.32 nA. The remarkable fact about this image is that the force constant of the cantilever was only 16 N/m. A commonly observed phenomenon in an AFM experiments is that the cantilever jumps into contact when the force gradient of the attractive interaction between tip and sample exceeds the force gradient of the cantilever. Therefore, stable tunneling between an integrated cantilever tip and a sample is only possible if the force gradient of the attractive interaction between tip and sample is smaller than the force gradient of the cantilever.

The attractive interaction between a silicon tip and a silicon sample is composed of a van der Waals and an electrostatic term. The van der Waals force gradient at a distance D between a spherical tip with radius R and a flat surface is given by[21]

$$\frac{\partial F(D)}{\partial D} = \frac{AR}{3D^3}. \tag{1}$$

Here, A denotes the Hamaker constant and its order of magnitude is $A = 10^{-19}$ J for most solids in vacuum.[14]

A rough approximation for the electrostatic force gradient between a spherical tip of radius R at a distance D and a potential difference U to a flat surface derived by applying elementary electrostatics is given by

$$\frac{\partial F}{\partial D} = \epsilon_0 \frac{U^2 R^2}{D^3}. \tag{2}$$

For typical tunneling parameters of $D = 4$ Å and $U = 2$ V, the electrostatic force gradient is 50 N/m for a tip radius of 40 Å. The van der Waals contribution is less than the electrostatic contribution and can be neglected. Knowing the force constant of the piezoresistive cantilever to be 16 N/m, we conclude that the radius of the tip is less than 40 Å.

The fluctuations in force measured between the piezoresistive cantilever and the tip during imaging was smaller than the resolution of the force measurement (3 nN for a bandwidth between 0 Hz and 10 kHz). Cross-sectional line measurements of the Si(111) 7×7 adatom and corner hole features in this image show resolution comparable to conventional STM measurements using tungsten tips.

These experiments represent demonstration of STM imaging using an AFM cantilever structure in UHV. This breakthrough means the piezoresistive cantilever has the potential to perform simultaneous AFM/STM measurements on the same area of the sample and the ability to collect $I-V$ curves during AFM measurements without the necessity of changing probes.

IV. DISCUSSION

We have demonstrated a unique ultrahigh vacuum scanning probe microscope capable of scanning tunneling microscopy, contact atomic force microscopy, and noncontact atomic force microscopy. The microscope utilizes a piezoresistive cantilever detection scheme that eliminates the need for the precision alignment required by conventional optical lever AFM systems. We have shown atomic resolution imaging in both scanning tunneling and atomic force microscopy modes. A new technique using the piezoresistive cantilever for both AFM and STM imaging is presented.

ACKNOWLEDGMENTS

[1] G. Binnig, H. Rohrer, Ch. Gerber and E. Weibel, Appl. Phys. Lett. **62**, 834 (1986); Phys. Rev. Lett. **49**, 57 (1992); Physica **109/110b**, 2075 (1982).
[2] F. J. Giessibl, Ch. Gerber, and G. Binnig, J. Vac. Sci. Technol. B **9**, 984 (1991).
[3] E. Meyer and H. J. Guentherodt (private communication).
[4] G. Neubauer, S. R. Cohen, G. M. McClelland, D. Horne, and C. M. Quate, Rev. Sci. Instrum. **61**, 2296 (1990).
[5] F. J. Germann, S. R. Cohen, G. Neubauer, G. M. McClelland, H. Seki, and D. Coulman, J. Appl. Phys. **73**, 163 (1993).
[6] G. Meyer and N. M. Amer, Appl. Phys. Lett. **53**, 1045 (1988).
[7] L. Howald, H. Rudin, and H.-J. Guentherodt, Rev. Sci. Instrum. **63**, 3909 (1992); L. Howald, E. Meyer, R. Luethi, H. Haefke, R. Overney, H. Rudin, and H.-J. Guentherodt, Appl. Phys. Lett. **63**, 117 (1993).
[8] L. Howald, H. Haefke, R. Luethi, E. Meyer, G. Gerth, H. Rudin, and H.-J. Guentherodt, Phys. Rev. B (in press) discussed UHV AFM measurements of NaF crystals.

Tunneling and force microscope

[9] M. Tortonese, R. C. Barrett, and C. F. Quate, Appl. Phys. Lett. **62**, 834 (1993) and M. Tortonese, Ph.D. thesis, Stanford University, 1993.

[10] S. I. Park, Ph.D. thesis, Stanford University, 1986.

[11] A. R. Smith, S. Gwo, and C. K. Shih (unpublished).

[12] G. Binnig and D. P. E. Smith, Rev. Sci. Instrum. **57**, 1688 (1986).

[13] See Ref. 9.

[14] Marco Tortonese (private communication).

[15] Analog Devices, P.O. Box 9106, Norwood, MA 02062, USA.

[16] D. P. E. Smith, Rev. Sci. Instrum. (to be published).

[17] *Landolt-Boernstein, Numerical Data and Functional Relationships in Science and Technology*, edited by O. Madelung, New Series, Vol. 17a, (Springer, Berlin, 1982).

[18] See Ref. 9.

[19] T. R. Albrecht, P. Gruetter, D. Horne, and D. Rugar, J. Appl. Phys. **69**, 668 (1991).

[20] A more detailed discussion of non-contact AFM in vacuum can be found in F. J. Giessibl, Jpn. J. Appl. Phys. (to be published).

[21] J. N. Israelachvili, *Intermolecular and Surface Forces* (Academic, London, 1985), Sec. 11.1.